

Optimization of the Fixed Target Beamline for the Neutron Therapy Facility

Kelly J. Vazquez

Department of Physics

North Central College

Naperville, IL, 60585

Supervisor: Dr. Thomas K. Kroc

Accelerator Division

Fermi National Accelerator Laboratory

Batavia, IL 60510-5011

Summer Internships in Science & Technology (SIST) Program

August, 2015

Fermi National Accelerator Laboratory



Table of Contents

Introduction	3
Introduction: Objective.....	4
Introduction: Background.....	4
Overview of the NTF Beamline	5
Accelerator Programming Background	6
Accelerator Elements	6
Optical Analogy	7
Applications of Linear Algebra.....	7
TWISS Parameters.....	8
OptiMX	8
OptiMX Background.....	8
Input Files	9
Output Files	10
MAD8	11
MAD8 Background	11
Input Files	11
Output Files	12
SURVEY Command.....	13
Methods of Calculating Misalignment	13
Linear Fits & Intersection Points.....	13
Finding the Bend Center	14
MAD ERROR Command	15
Results	15
Conclusions & Future Work	16
Calculate Variance Downstream.....	17
Verify Misalignment Upstream	18
Propose Optimization	19
Acknowledgements	19
References	20

Abstract

A branch off of Fermilab's linear accelerator (Linac), the existing fixed-target beamline bends a combined 90° off of the Linac. This line served as the source of neutrons for irradiation in the Neutron Therapy Facility (NTF) that ceased its treatment of cancer patients in 2013. The beamline is still fully operational; however, due to data previously collected and analyzed we proposed that the beam may be entering the accelerator line off-axis. Therefore, the purpose of our project was to determine if the beamline was misaligned and if so, in what ways it could be optimized such that the proton beam entered the NTF line in the bend center of the magnets. Using a recent alignment survey analysis that occurred during a previous shutdown paired with the accelerator design programs MAD8 (Methodical Accelerator Design, version 8.0) and OptiMX, we were able to simulate the beam through the line. Using these simulations we were able to determine the components of the line that were off-axis and would need further adjustment. Ultimately, this will allow us to verify that the center of the target is hit.

1. Introduction

1.1 Introduction: Objective

Currently in the facility there is an existing fully operational, fixed-target beamline which served as the source of neutrons for irradiation in the Neutron Therapy Facility (NTF) that ceased its treatment of cancer patients in 2013. Although NTF is no longer treating cancer patients, the beamline is used for various radiation purposes such as cancer cell research, plant irradiation, and other applications in industry. Because the beamline is still operational, the maintenance and alignment of the machine is still of significant importance. The graph of data that was previously collected and analyzed of the beam profile depicts transverse motion in the beamline that indicates quadrupole steering (Fig.1). Due to evidence of quadrupole steering which points to probable misalignment, we proposed that the beam may be entering off-axis.

The purpose of our project was: 1) reduce the quadrupole magnet currents in the beamline, 2) verify misalignment in the existing fixed-target beamline, and 3) if misaligned, optimize the beamline such that it enters the NTF line on-axis.

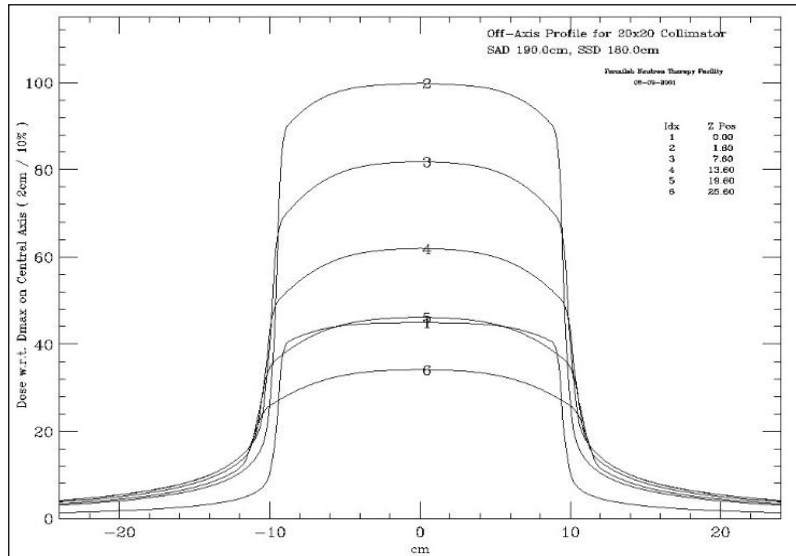


Figure 1. Beam distribution plot using 20x20 collimator

1.2 Introduction: Background

As a leader in the area of particle physics, Fermi National Accelerator Laboratory uses a series of accelerators to create powerful beams of particles. In order to create the proton beams needed for various experiments, Fermi's linear particle accelerator accelerates negatively charged hydrogen ions. These ions are produced from the 750keV H⁻ ion source in the Linac's pre-accelerator. Approximately 500 feet long, the Linac accelerates the proton beam up to 400 million electron volts (MeV) using a series of linear radio frequency accelerating tanks. Once it reaches the end of the Linac, the 400 MeV proton beam continues on to other accelerators across the lab.

In addition to particle physics, particle accelerators have significant applications to medicine. Shortly after the discovery of neutrons, Dr. Robert Stone began experimenting with neutron therapy for cancer patients in 1938. In the 1970s, Dr. Robert Wilson of Fermilab created the Neutron Therapy Facility (NTF), and on September 7, 1976 NTF treated their first patient.

2. Overview of the NTF Beamline



Figure 2. [2.1 Top] Panoramic view of the entrance to the NTF fixed-target beamline in between the Linac tanks 4 and 5 with the 58° bending dipole shown. [2.2 Bottom] Entrance to tank 5 from the 58° dipole.



As seen above (Fig. 2.1), the NTF fixed-target beamline begins at the end of tank 4 of the Linac. At this point, the proton beam is bent by a 58° rectangular dipole bending magnet that marks the entrance of the beamline. In order to focus the beam, quadrupole magnets are placed in an optically focus-defocus pattern to account for the quadrupole's ability to only focus in one plane and defocus in the other. Following the first two quadrupole magnets, the beam reaches another rectangular bending dipole magnet of 32° to complete the perpendicular bend necessary to reach the target in the patient treatment room. To continue the focus of the beam until the Beryllium target, a sequence of 5 additional focusing quadrupoles completes the beamline. Following the generation of neutrons at the target, the beam enters the collimator until it exits to the object being irradiated.

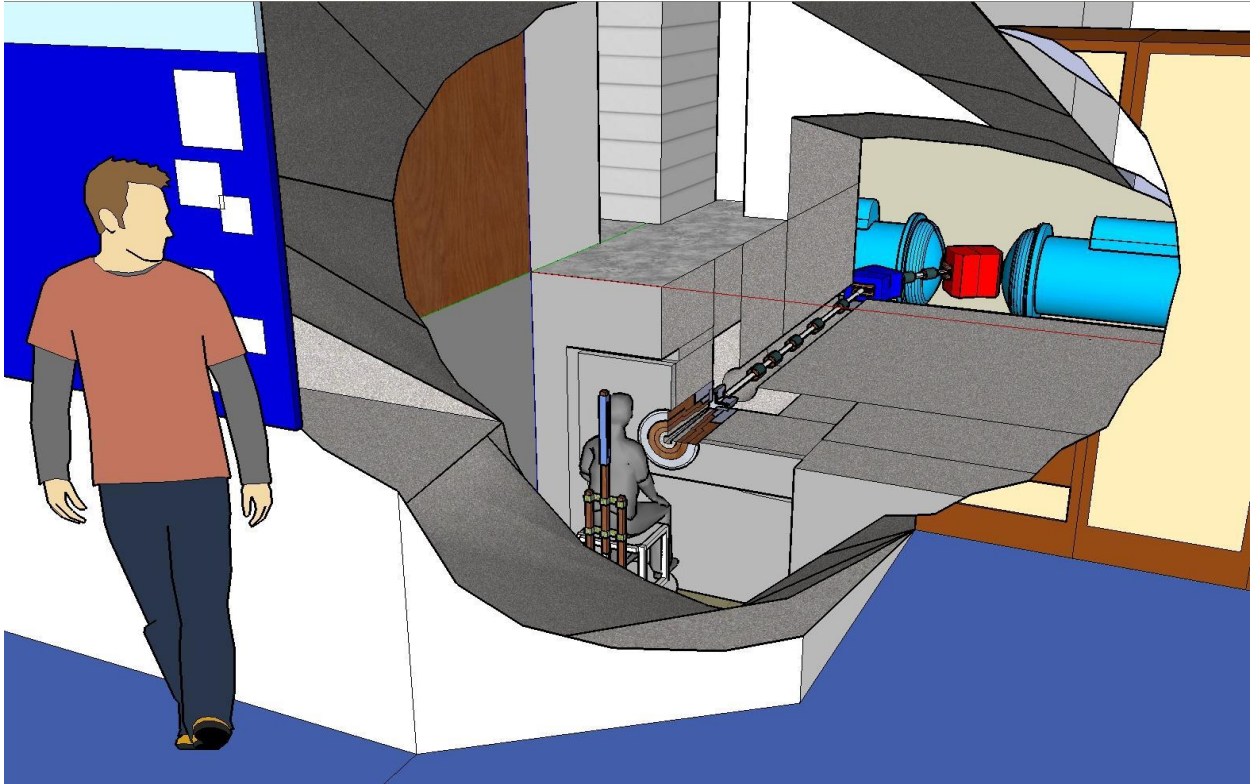


Figure 3. Cutaway view of the NTF fixed-target beamline from the Linac tank 4 to the patient treatment room.

3. Accelerator Programming Background

3.1 Accelerator elements

One of the fundamental types of components within an accelerator beamline are the magnets. There are two styles that are used in the NTF beamline due to our need for both focusing and bending in order to complete the perpendicular bend off of the Linac line to the target, and the need to focus the beam precisely on the Beryllium target. The first type of magnet we will discuss are the rectangular bending dipole magnets, in our case this refers to the 58° and 32° magnets in the line. Often called “bending magnets,” a dipole magnet has 2 poles. This magnet is used to realize bends in the design trajectory of the particle beam. In addition to dipoles, the other type of magnets in our beamline are quadrupole magnets. Often referred to as “focusing magnets,” a quadrupole magnet has 4 poles. Due to the 4 poles it contains, a quadrupole which defocuses in one plane focuses in the other. Therefore, at the same time that a quadrupole magnet is

horizontally focusing, the magnet is simultaneously defocusing in the vertically, and vice-versa.

3.2 Optical Analogy

As mentioned above, this inability of the quadrupole magnets to focus in both planes requires us to array the quadrupole magnets in a focus-defocus pattern (often called FODO) in order to keep the beam on-axis. Often when dealing with the optics of accelerators, the analogy to the combination of concave and convex lenses for optical focusing is made.

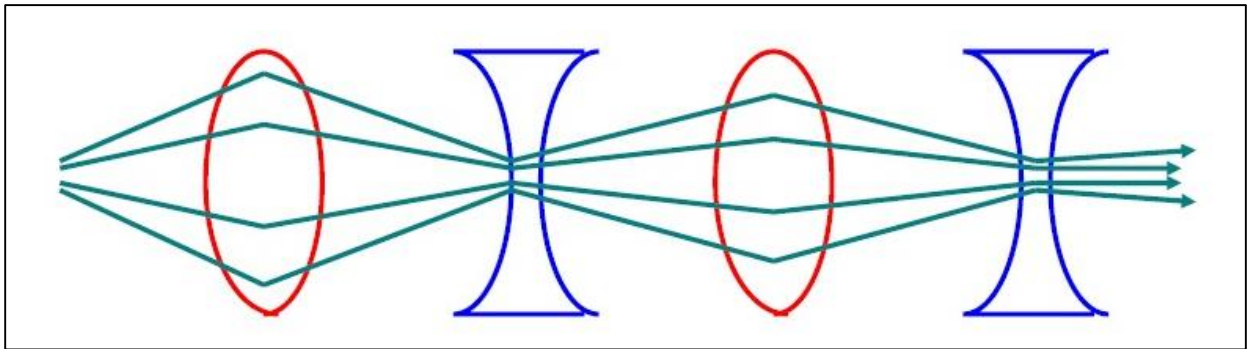


Figure 4. Schematic of the FODO effect using concave & convex optical lenses

3.3 Linear Algebra Applications

There are two key components of Accelerator programming: lattice matrices and TWISS parameters. To begin, there are extensive applications of linear algebra within the lattice structure of the beamline. Below are the matrix elements of both the focusing and defocusing quadrupoles:

$$\mathbf{M}_F = \begin{bmatrix} \cos(\kappa_0 l) & \frac{1}{\kappa_0} \sin(\kappa_0 l) \\ -\kappa_0 \sin(\kappa_0 l) & \cos(\kappa_0 l) \end{bmatrix}, \quad \mathbf{M}_D = \begin{bmatrix} \cosh(|\kappa_0| l) & \frac{1}{|\kappa_0|} \sinh(|\kappa_0| l) \\ |\kappa_0| \sinh(|\kappa_0| l) & \cosh(|\kappa_0| l) \end{bmatrix}$$

Figure 5. Matrix elements for focusing and defocusing quadrupoles prior to implementation of Thin Lens Approx.

These look quite involved; yet, the thin lens approximation can be implemented. Once the thin lens approximation is used we are left with the matrix element pictured

below (Fig. 6). However, the sign of the lower left element is flipped depending on whether or not the quadrupole is focusing or defocusing.

$$\mathbf{M}_{F(D)} = \begin{bmatrix} 1 & 0 \\ -\frac{1}{f} & 1 \end{bmatrix}$$

Figure 6. Matrices for focusing and defocusing quadrupoles with application of thin lens approximation

3.4 TWISS Parameters

As mentioned previously, the second key component of accelerator programming are the TWISS parameters. The beam shape is modeled as an ellipse that fluctuates in size and shape as it travels along the beamline. The parameters of the beam size and shape are commonly referred to as the TWISS parameters of the machine. These parameters are broken into the $\beta_{x,y}$ and $\alpha_{x,y}$ components of the beam ellipse. The $\beta_{x,y}$ components are a function of the horizontal and vertical size of the beam. In essence, the width of the beam can be found with these parameters. The $\alpha_{x,y}$ components of the beam ellipse are a function of the change in the tilt of the ellipse. Therefore, the $\alpha_{x,y}$ parameters allow the user to determine the angle of the beam.

4. OptiMX

4.1 OptiMX Background

In order to calculate the misalignment of the beamline, it was necessary that we create a simulation of the beam through the line using accelerator software. The first program that we implemented was OptiMX. OptiM is a computer program developed and maintained by Fermi physicists that is aimed at assisting with the linear optics design of particle accelerators. The program allows the user to compute dispersion and beam sizes with linear optics calculations that are done based on a 6 dimensional transfer matrix. In addition, the program allows the user to output and plot betatron functions (Twiss Parameters).

4.2 Input Files

OptiMx has been used in previous years to create simulations of the NTF beamline; therefore, some existing input files were present. However, during a recent shutdown the beamline was surveyed. This survey analysis provided the coordinates for each of the elements in the beamline according to a local coordinate system. Using the data from the survey paired with the existing input files, we were able to create updated OptiMX input files with lengths of the magnets and drifts corrected with the most recent survey data. OptiMX requires the initial length, magnetic gradient, and tilt angle of each of the elements of the beamline. In addition, it requires the initial energy and momentum value, the type of particle, mass of the particle, and the initial TWISS parameters. The energy of the protons entering the NTF beamline are at 66 MeV. Using this energy value with the equations pictured below (Fig.7), we calculated the momentum of the particles and input that value into OptiMX.

$$E = m_0c^2 + K$$

$$E^2 = p^2c^2 + m_0c^2$$

$$p = \sqrt{\frac{(E^2 - m_0c^2)}{c^2}}$$

Figure 7. Equations for calculation of momentum for OptiMX input

Once the initial parameter values were entered, the elements of the beamline were arranged to form the beamline.

The screenshot shows the OptiMX (LINE) - [NTFbeamline_long.opt] window. The interface includes a menu bar (File, Edit, Search, Fitting, Tools, View, View 4D, SpaceCharge, Window, Preferences, Help) and a toolbar. The main area displays a list of beamline elements with their parameters. The elements are listed in a table-like format with columns for element names and various physical parameters.

Element Name	Length [cm]	Magnetic Gradient [kg/cm]	Tilt [deg]	Other Parameters
q4_19	47.3761			
q4_20	47.6557	G[kg/cm]=SGT4_20	Tilt[deg]=0	
q4_21	47.9337	G[kg/cm]=SGT4_21	Tilt[deg]=0	
q4_22	48.2101	G[kg/cm]=SGT4_22	Tilt[deg]=0	
q4_23	48.4851	G[kg/cm]=SGT4_23	Tilt[deg]=0	
q4_24	48.7585	G[kg/cm]=SGT4_24	Tilt[deg]=0	
q4_25	49.0304	G[kg/cm]=SGT4_25	Tilt[deg]=0	
q4_26	49.3097	G[kg/cm]=SGT4_26	Tilt[deg]=0	
q4_27	49.5694	G[kg/cm]=SGT4_27	Tilt[deg]=0	
q4_28	49.8366	G[kg/cm]=SGT4_28	Tilt[deg]=0	
q4_29	50.1024	G[kg/cm]=SGT4_29	Tilt[deg]=0	
q4_30	50.3667	G[kg/cm]=SGT4_30	Tilt[deg]=0	
h4_out	1.422	Shape=1	OffsetX[cm]=0	OffsetY[cm]=0 Tilt[deg]=0
KS58	1.422	Shape=1	OffsetX[cm]=0	OffsetY[cm]=0 Tilt[deg]=0
G58	1.422	Shape=1	OffsetX[cm]=0	OffsetY[cm]=0 Tilt[deg]=0
D58	1.422	Shape=1	OffsetX[cm]=0	OffsetY[cm]=0 Tilt[deg]=0
o58_1	25.4	B[kg]=SB58Ref	Angle[deg]=\$FaceAngle58	EffLen[cm]=\$EffL58 Tilt[deg]=0
o58_2	2.64	B[kg]=SB58Ref	G[kg/cm]=\$G58	
kv	12.5	B[kg]=SGVICTF	Tilt[deg]=90.	
qc02	2.64	B[kg]=SGC01	Tilt[deg]=0	OfsX[cm]=\$SPlateOffx OfsY[cm]=\$SPlateOffy
o58_4	20.27	B[kg]=SGC02	Tilt[deg]=0	OfsX[cm]=\$SPlateOffx OfsY[cm]=\$SPlateOffy
h32	1.905	Shape=1	OffsetX[cm]=0	OffsetY[cm]=0 Tilt[deg]=0
G32	1.905	Shape=1	OffsetX[cm]=0	OffsetY[cm]=0 Tilt[deg]=0
D32	1.905	Shape=1	OffsetX[cm]=0	OffsetY[cm]=0 Tilt[deg]=0
h32_out	1.905	Shape=1	OffsetX[cm]=0	OffsetY[cm]=0 Tilt[deg]=0
o32_1	40.8	B[kg]=SB32Ref	Angle[deg]=\$FaceAngle32	EffLen[cm]=\$EffL32 Tilt[deg]=0
kh1	20.	B[kg]=SB32Ref	G[kg/cm]=\$G32	
o32_2	3.97	Shape=1	OffsetX[cm]=0	OffsetY[cm]=0 Tilt[deg]=0
oc03	15.4	B[kg]=SGKH1	Tilt[deg]=0.	
oc03_1	20.	B[kg]=SGC03	Tilt[deg]=0	OfsX[cm]=\$SchuteOffx OfsY[cm]=\$SchuteOffy
oc03_2	20.	B[kg]=SGC03	Tilt[deg]=0	OfsX[cm]=\$SchuteOffx OfsY[cm]=\$SchuteOffy
qc04	20.	B[kg]=SGKH2	Tilt[deg]=0.	
oc04	49.53	B[kg]=SGC04	Tilt[deg]=0	OfsX[cm]=\$SchuteOffx OfsY[cm]=\$SchuteOffy
oc05	39.37	B[kg]=SGC05	Tilt[deg]=0	OfsX[cm]=\$SchuteOffx OfsY[cm]=\$SchuteOffy
oc06	26.67	B[kg]=SGC06	Tilt[deg]=0	OfsX[cm]=\$SchuteOffx OfsY[cm]=\$SchuteOffy
oc07	26.67	B[kg]=SGC07	Tilt[deg]=0	OfsX[cm]=\$SchuteOffx OfsY[cm]=\$SchuteOffy
hc7_out	1.905	Shape=1	OffsetX[cm]=0	OffsetY[cm]=0 Tilt[deg]=0
oc07_tant	65.24	Shape=1	OffsetX[cm]=0	OffsetY[cm]=0 Tilt[deg]=0
htant	0.7938	Shape=1	OffsetX[cm]=0	OffsetY[cm]=0 Tilt[deg]=0
oc_tant_tgt	0.9525	Shape=1	OffsetX[cm]=0	OffsetY[cm]=0 Tilt[deg]=0
htant	1.27	Shape=1	OffsetX[cm]=0	OffsetY[cm]=0 Tilt[deg]=0

Figure 8. OptiMX Input file

4.3 Output Files

OptiMX allows the user to output a plot of the $\beta_{x,y}$ TWISS parameters as a function of distance along the beamline, s . In addition, OptiMX plots the dispersion in x and y as a function of distance. The program also generates a schematic of the beamline above the $\beta_{x,y}$ plot that depicts the variation between quadrupoles and dipoles and allows the user to visualize the TWISS parameters at each of the elements of the beamline.

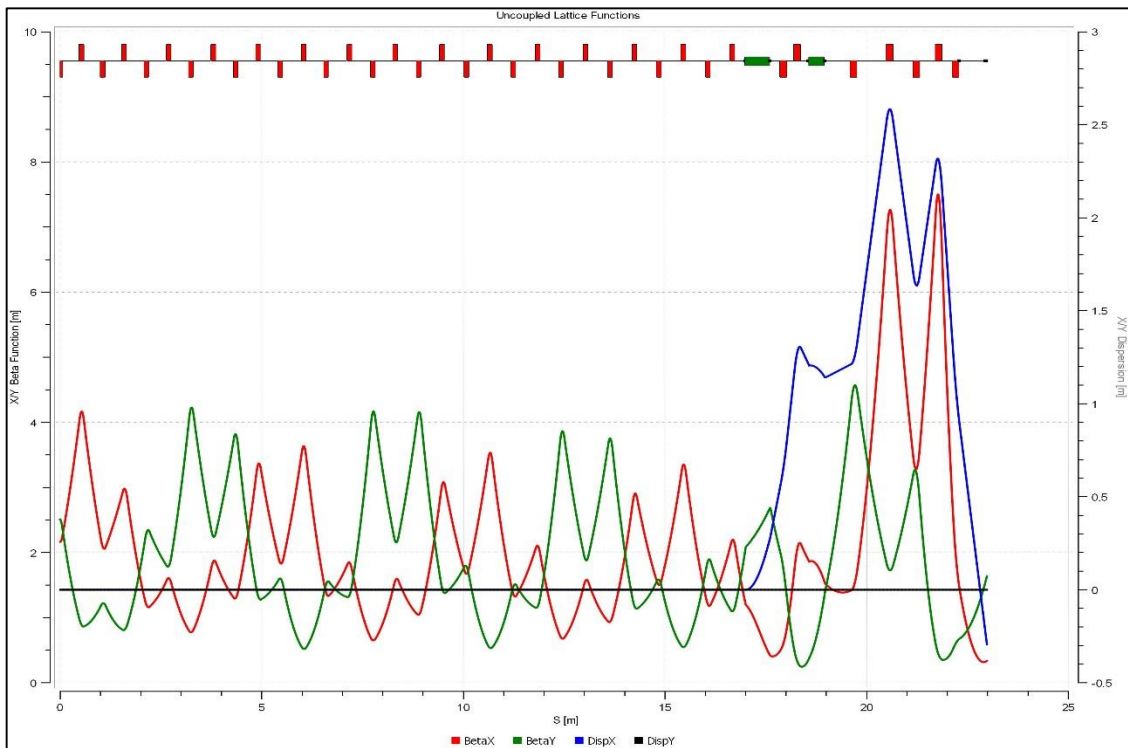


Figure 9. OptiMX plot of the TWISS parameters $\beta_{x,y}$ vs. s

5. MAD8

5.1 MAD Background

Although OptiMX allows the user to compute and plot the TWISS parameters of the machine, another accelerator program, Methodical Accelerator Design or MAD (v. 8.0), was used. Developed by CERN physicists for accelerator design and simulation, MAD is an ongoing project that is at the forefront of particle accelerator design and

simulation. Although similar in purpose to OptiMX, MAD is one of the standard scripting languages for accelerators and can perform many functions that OptiMX simply cannot. A newer version, MAD-X, is currently maintained and operated by CERN and has replaced MAD8. However, due to the ease of code entry and output analysis, MAD8 was used for this project.

5.2 Input Files

The existing OptiMX files were first exported to MAD8 input files in order to simulate the beamline with the program. One of the features of the MAD8 program is the ability to organize input files according to elements and therefore generate a very clean input file. This allows the user freedom to input the elements of the beamline quite simply.

```

79 !*****NTF Line Quads*****
80
81 q4_30: QUADRUPOLE, L= 0.1138, K1=13.64609376
82 qc01: QUADRUPOLE, L= 0.1646, K1= -7.92782537
83 qc02: QUADRUPOLE, L= 0.1646, K1= 11.75706379
84 qc03: QUADRUPOLE, L= 0.1646, K1= -7.321122559
85 qc04: QUADRUPOLE, L= 0.1646, K1= 7.755709743
86 qc05: QUADRUPOLE, L= 0.1646, K1=-11.44731296
87 qc06: QUADRUPOLE, L= 0.1646, K1= 12.5266174
88 qc07: QUADRUPOLE, L= 0.1646, K1= -8.304913327
89
90 !*****NTF Line Drifts*****
91
92 o4_30: DRIFT, L=0.23971
93 o58_1: DRIFT, L=0.254
94 o58_2: DRIFT, L=0.0264
95 o58_3: DRIFT, L=0.0264
96 o58_4: DRIFT, L=0.1927
97 o32_1: DRIFT, L=0.408
98 o32_2: DRIFT, L=0.0397
99 oc03_1:DRIFT, L=0.154
100 oc03_2:DRIFT, L=0.3572
101 oc04: DRIFT, L=0.4953
102 oc05: DRIFT, L=0.3937
103 oc06: DRIFT, L=0.2667
104 oc07_tant: DRIFT, L= 0.6524
105 oc_tant_tgt: DRIFT, L=0.009525
106 oc_tgt:DRIFT, L=0.0127
107
108 !*****NTF Line Bends*****
109
110 D58: SBEND, L= 0.4091987, ANGLE=1.0122942844
111 , E1=0.5061454831 , HGAP=0.01891964739, FINIX=0.5 &
112 , E2=0.5061454831 , HGAP=0.01891964739, FINIX=0.5
113 D32: SBEND, L= 0.3954221, ANGLE=0.5585057914
114 , E1=0.2792526803 , HGAP=0.01572596577, FINIX=0.5 &
115 , E2=0.2792526803 , HGAP=0.01572596577, FINIX=0.5
116
  
```

Figure 10. MAD8 Input Files [10.1 Top] Input by elements. [10.2 Bottom] Input of Beamline.

```

136
137 !*****Beamline from Linac tank 4 to NTF line*****
138
139 NTFLINE: LINE=(q4_1, o4_1, q4_2, o4_2, q4_3, o4_3, q4_4, o4_4, q4_5, o4_5, &
140 q4_6, o4_6, q4_7, o4_7, q4_8, o4_8, q4_9, o4_9, q4_10, o4_10, q4_11, o4_11, &
141 q4_12, o4_12, q4_13, o4_13, q4_14, o4_14, q4_15, o4_15, q4_16, o4_16, &
142 q4_17, o4_17, q4_18, o4_18, q4_19, o4_19, q4_20, o4_20, q4_21, o4_21, &
143 q4_22, o4_22, q4_23, o4_23, q4_24, o4_24, q4_25, o4_25, q4_26, o4_26, &
144 q4_27, o4_27, q4_28, o4_28, q4_29, o4_29, q4_30, o4_30, h4_out, K58, D58, &
145 o58_1, qc01, o58_2, kv, o58_3, qc02, o58_4, K32, D32, h32_out, o32_1, kH1, &
146 o32_2, qc03, oc03_1, kH2, oc03_2, qc04, oc04, qc05, oc05, qc06, oc06, qc07, &
147 hc7_out, oc07_tant, htant, oc_tant_tgt, htgt, oc_tgt)
148
149 use,ntfline
150
151 twiss, save, couple, betx= 2.1649, alfx= 0.04022, &
152 bety= 2.5102, alfy= 0.29886, &
153 dx= 0, dpx= 0, &
154 dy= 0, dpy= 0, TAPE=line.twiss
155
156 survey, save, z0=0, x0=0, TAPE=line.survey
157 plot, table=twiss, colour=100, haxis=s, vaxis1=betx, bety, &
158 vaxis2=dx
159 plot, table=twiss, colour=100, haxis=s, vaxis1=betx, bety, &
  
```

5.3 Output Files

Once the files had been properly exported to MAD8, we verified that all of the TWISS parameters matched those calculated in OptiMX. In addition, we generated plots of the $\beta_{x,y}$ functions as a function of distance and verified that they matched the OptiMX output.

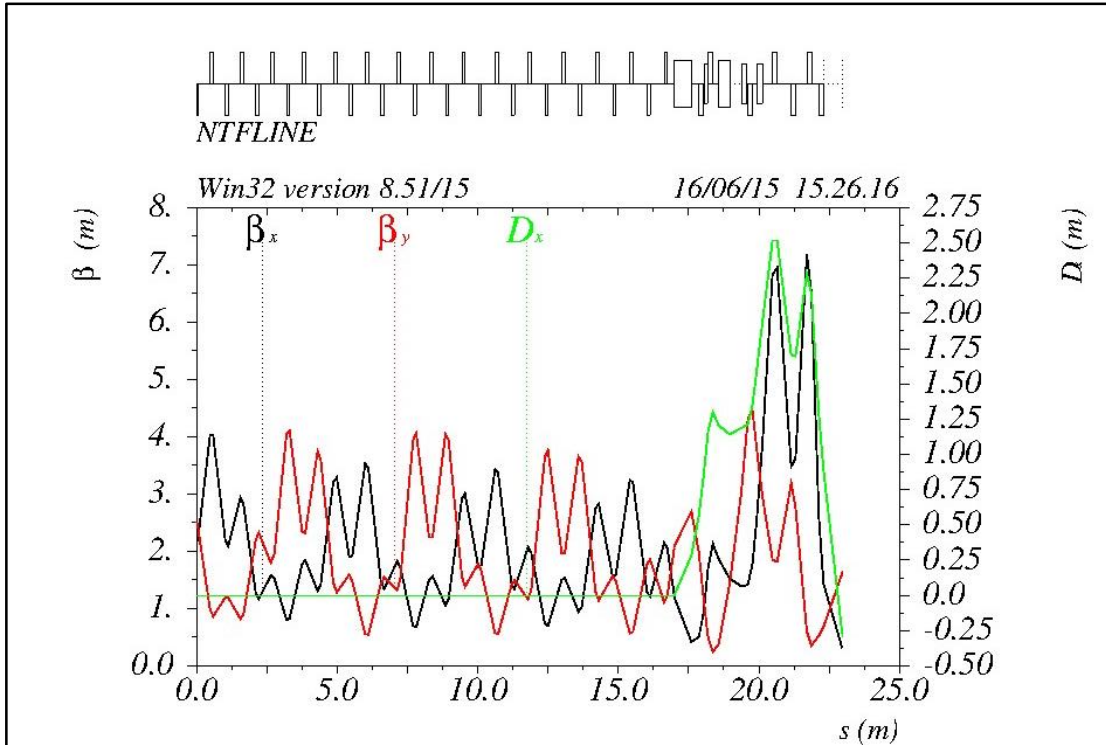


Figure 11. MAD8 plot of the TWISS parameters $\beta_{x,y}$ vs. s

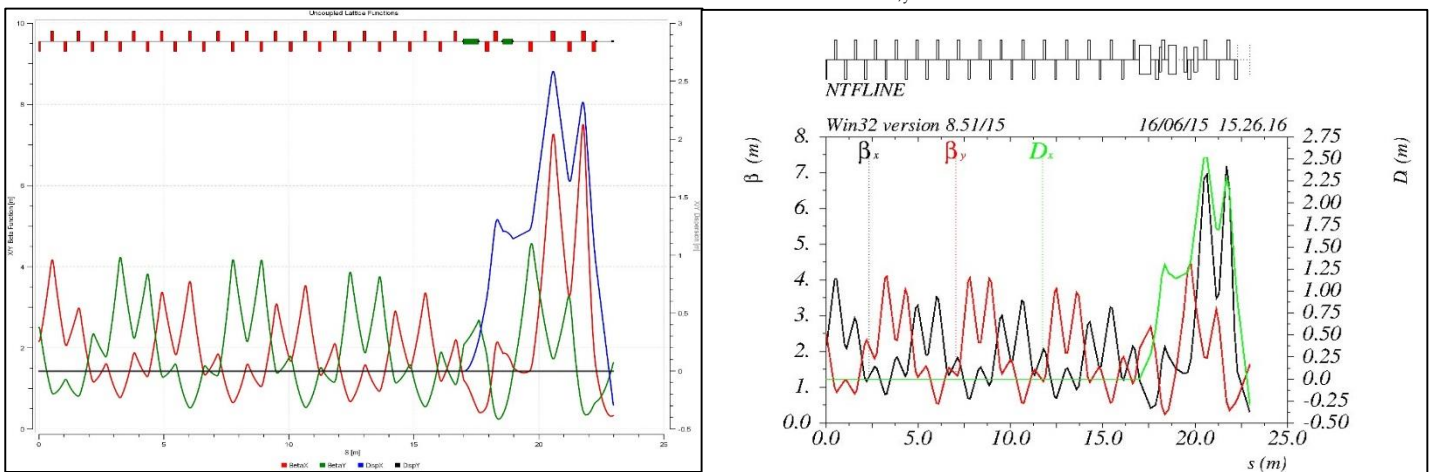


Figure 12. [Left] OptiMX $\beta_{x,y}$ plot and [Right] MAD8 $\beta_{x,y}$ plot

5.4 SURVEY command

Using the Survey command, we were able to output a geometrical survey of the elements that allowed us to compare physical lengths to effective.

```

81 -----
82 1 Survey. SURVEY line: NTFLINE "MAD" Version: 8.51/15 Run: 21/07/15 09.36.55
83 symm: F super: 1 range: #S/#E
84 ----- page 1
85 -----
86 ELEMENT SEQUENCE I POSITIONS I ANGL ES
87 pos. element occ. sum(L) arc I x y z I theta phi psi
88 no. name no. [m] [m] I [m] [m] [m] I [rad] [rad] [rad]
89 -----
90 begin NTFLINE 1 0.000000 0.000000 36.792000 0.000000 -0.012000 4.712477 0.000000 0.000000
91 1 DS8 1 0.583519 0.609199 36.281668 0.000000 0.270941 5.724771 0.000000 0.000000
92 2 OS8_1 1 0.837519 0.863199 36.147088 0.000000 0.486358 5.724771 0.000000 0.000000
93 3 QC01 1 1.002119 1.027799 36.059876 0.000000 0.625955 5.724771 0.000000 0.000000
94 4 OS8_2 1 1.028519 1.054199 36.045889 0.000000 0.648344 5.724771 0.000000 0.000000
95 5 KV 1 1.153519 1.179199 35.979658 0.000000 0.754356 5.724771 0.000000 0.000000
96 6 OS8_3 1 1.179919 1.205599 35.965670 0.000000 0.776746 5.724771 0.000000 0.000000
97 7 QC02 1 1.344519 1.370199 35.878458 0.000000 0.916343 5.724771 0.000000 0.000000
98 8 OS8_4 1 1.537219 1.562899 35.776358 0.000000 1.079771 5.724771 0.000000 0.000000
99 9 K32 1 1.547219 1.572899 35.771060 0.000000 1.088252 5.724771 0.000000 0.000000
100 10 DS2 1 1.937535 1.968335 35.663508 0.000000 1.463458 6.283277 0.000000 0.000000
101 11 OS2_1 1 2.345535 2.376335 35.663546 0.000000 1.871458 6.283277 0.000000 0.000000
102 12 KH1 1 2.545535 2.576335 35.663564 0.000000 2.071458 6.283277 0.000000 0.000000
103 13 OS2_2 1 2.585235 2.616035 35.663568 0.000000 2.111158 6.283277 0.000000 0.000000
104 14 QC03 1 2.749835 2.780635 35.663583 0.000000 2.275758 6.283277 0.000000 0.000000
105 15 OC03_1 1 2.903835 2.934635 35.663597 0.000000 2.429758 6.283277 0.000000 0.000000
106 16 KH2 1 3.103835 3.134635 35.663615 0.000000 2.629758 6.283277 0.000000 0.000000
107 17 OC03_2 1 3.461035 3.491835 35.663648 0.000000 2.989958 6.283277 0.000000 0.000000
108 18 QC04 1 3.625635 3.656435 35.663663 0.000000 3.151558 6.283277 0.000000 0.000000
109 19 OC04 1 4.120935 4.151735 35.663708 0.000000 3.646858 6.283277 0.000000 0.000000
110 20 QC05 1 4.285535 4.316335 35.663723 0.000000 3.811458 6.283277 0.000000 0.000000
111 21 OC05 1 4.679235 4.710035 35.663760 0.000000 4.205158 6.283277 0.000000 0.000000
112 22 QC06 1 4.843835 4.874635 35.663775 0.000000 4.369758 6.283277 0.000000 0.000000
113 23 OC06 1 5.110535 5.141335 35.663799 0.000000 4.636458 6.283277 0.000000 0.000000
114 24 QC07 1 5.275135 5.305935 35.663814 0.000000 4.801058 6.283277 0.000000 0.000000
115 end NTFLINE 1 5.275135 5.305935 35.663814 0.000000 4.801058 6.283277 0.000000 0.000000
116 -----
117 total length = 5.275135 arc length = 5.305935
118 error(x) = -0.112819E+01 error(y) = 0.000000E+00 error(z) = 0.481306E+01
119 error(theta) = 0.157080E+01 error(phi) = 0.000000E+00 error(psi) = 0.000000E+00
120 -----
121

```

Figure 13. SURVEY command output file

6. Methods for Calculating Misalignment

6.1 Linear Fits & Intersection Points

In order to determine if the beamline is on-axis as it accelerates downstream survey alignment data was used to develop equations that fit the coordinates of the elements within the local coordinate system of the beamline. In addition, the SURVEY command in MAD8 gave the θ_{Bearing} which allows the user to determine the equations for lines through individual elements. This allowed us to find equations for sections of the beamline: the line of the Linac, the line from the Linac extending through the 1st and 2nd quadrupoles, and the line through the last five quadrupoles to the target.

By comparing the equations that MAD8 generated to those calculated with the SURVEY data, we were able to verify that the coordinates were properly simulated in the MAD8 program. Using these equations the physical intersection points of these sectional lines with each other were calculated and the coordinates of the intersection points were found.

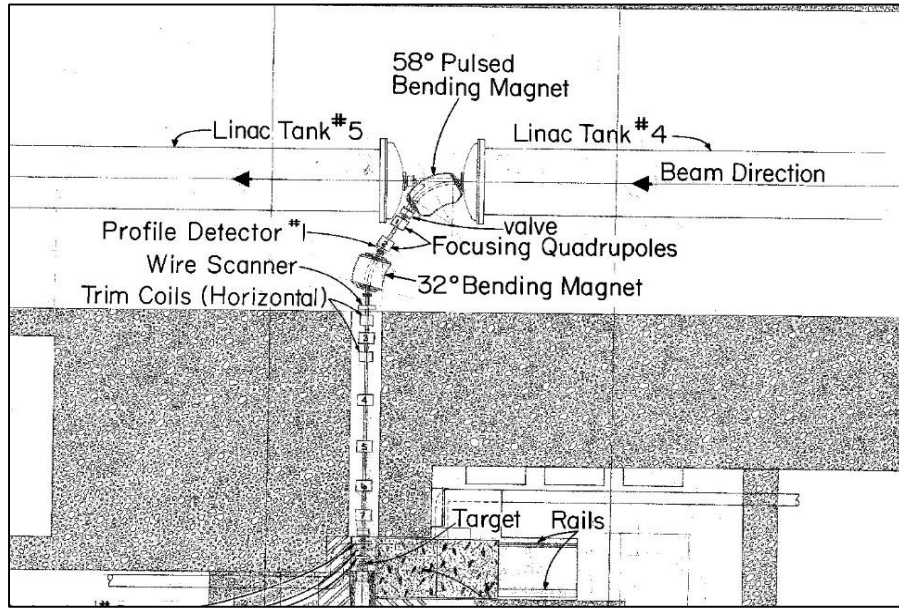


Figure 14. Layout of the NTF beamline

6.2 Finding the Bend Center

If the beamline is correctly aligned on-axis the beam should strike through the bend center of each of the rectangular bending dipole magnets. The bend center of a magnet is the intersection point between the lines through the entrance and exit of the magnet and the perpendicular bisector of the magnet.

To calculate the coordinates of the bend center and optimal trajectory of the beam, the equation of the perpendicular bisector of each of the dipoles was calculated using geometry. From this, the coordinates of the intersection point of the line bisecting the dipole and the line through the physical elements were found. Therefore, any variance found between the physical intersection point and the calculated bend center of the magnets revealed misalignment (Fig. 15).

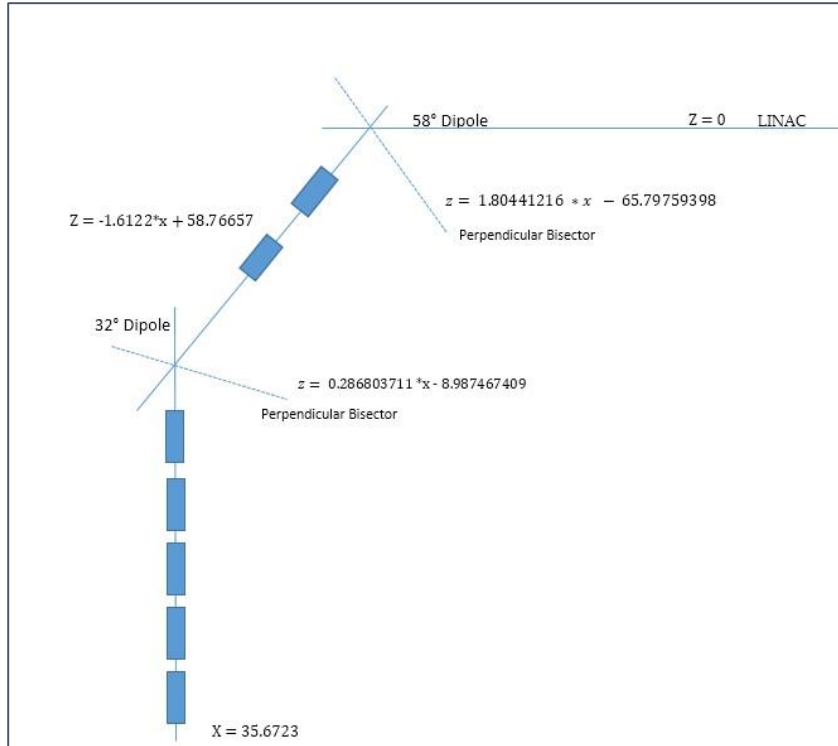


Figure 15. Schematic of the lines through the physical elements and the magnet's perpendicular bisectors and their equations

6.3 MAD ERROR Command

Another significant benefit of implementing MAD8 for simulating the beamline compared to OptiMX is the ERROR command function that OptiMX does not have. This command allows the user to assign calculated misalignments to specific elements in the beamline, and then simulate the beam through the line to find the misalignment that occurs downstream. Therefore, we entered the misalignment that was found in both the 58° and 32° dipoles, and then simulated the off-axis beam through the line to calculate a total misalignment.

```

55
56 use,ntfline
57 print,range=ntfline
58
59
60 !SELECT, flag=error, D58
61 !EALIGN,DS=0.01393
62
63
64 SELECT, flag=error, D32
65 EALIGN,DS=0.01170
66 EPRINT, RANGE=NTFLINE
67

```

Figure 16. Implementation of the ERROR command for the 58° and 32° dipoles

7. Results

Following a successful conversion and exportation from OptiMX to MAD8 for the input files, we were able to compare the output to that of the alignment survey data collected previously. After finding the linear equations through the different sections of the beamline, we calculated the intersection points of the existing lines with the perpendicular bisector of the magnets and found the misalignment error. By assigning the individual misalignments to the dipole elements with the ERROR command, we were able to simulate the off-axis beam till the 7th quadrupole and find the total misalignment downstream (Table 1).

	Distance(cm)**
Misalignment in 32°	1.17022
Misalignment in 58°	1.39255
Total Misalignment	1.34487

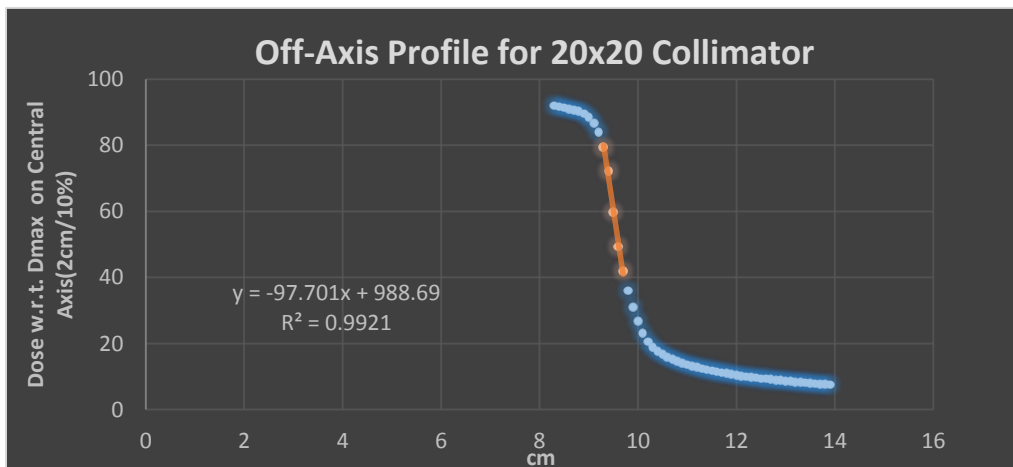
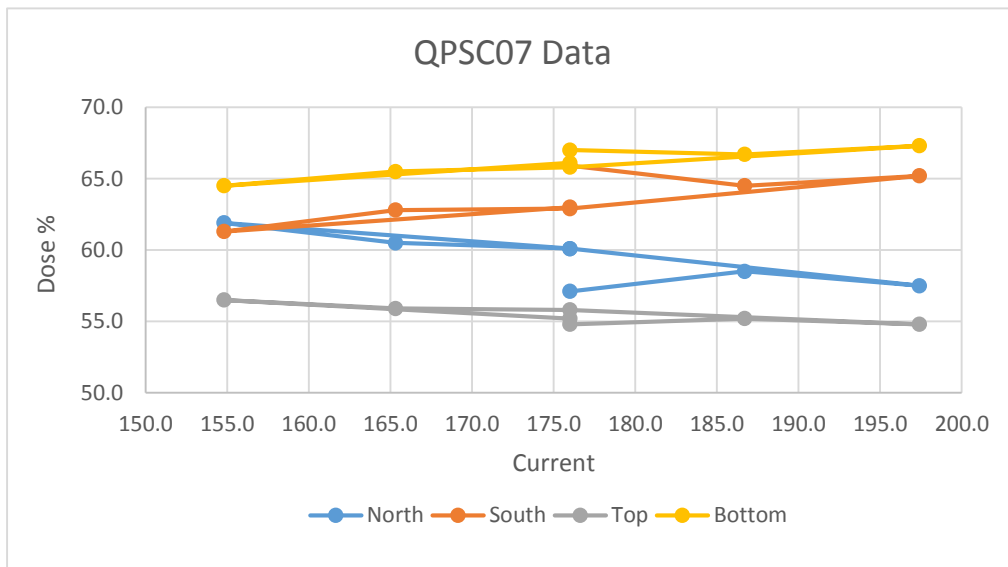
Table 1. Final results for individual element misalignments and the total misalignment downstream

8. Conclusions & Future Work

8.1 Calculate Variance Downstream

Prior to moving any of the elements to realign the beamline on-axis, we must verify the MAD error alignment output of a misalignment of 0.0134487 meters

upstream. In order to do this, we are using values collected at the target showing the off-axis beam distribution and working back upstream to verify the calculated misalignment with the existing data. As pictured below (Fig. 17.1), the data for quadrupole 7 shows the change in dose percentage as a function of current. As pictured in the introduction (Fig.1), the graph of the beam profile showing the transverse motion of the beam indicates quadrupole steering in the beamline. Using a portion of the profile data as pictured in Figure 17.2 we calculated an equation (Fig. 17.3) for the “fall-off” pictured in the graph that correlates to the motion of the beam. By rearranging the equation and solving for x , the x -coordinates dictate the position of the beam downstream related to the change in the dose percentage (current variation). Therefore, by inserting various values of “ y ”, or current percentage, from the quadrupole 7 data (Fig. 17.1), we can use the equation to find the position with the x -coordinates (Fig. 17.3).



$$y = -97.701x + 988.69$$

$$x = (y - 988.69) / -97.701$$

Figure 17. [17.1 Top] Plot of dose percentage as a function of current for Quadrupole 7. [17.2 Middle] Partial data plot of the off-axis beam profile with 20x20 collimator. [17.3 Bottom] Equations for the line to find x-coordinates.

8.2 Verify Misalignment Upstream

Using the x-coordinates calculated at the end of the beamline (as pictured in the schematic below) and geometrical ratios, the variance can be translated back upstream to the target prior to entering the collimator. Linear optics can then take the calculated values of misalignment at the target and move even farther upstream to see if the misalignment calculated at the 32° and 58° dipole elements can be replicated.

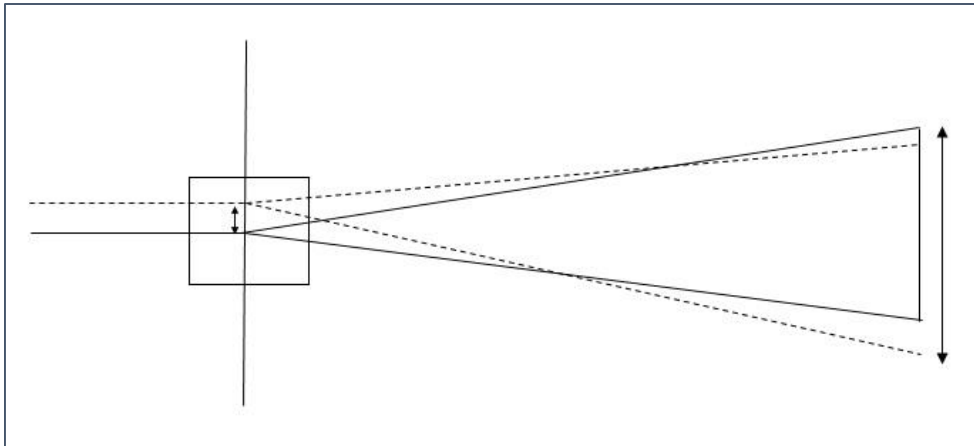


Figure. [Top] Schematic of the beam through the target and correlation of transverse motion back upstream [Bottom] Equations for the geometrical ratios for variance at the target

$$\frac{x - coordinate}{190cm} = \frac{y}{109cm}$$

8.3 Propose Optimization

Once the misalignment that has been calculated can be verified upstream and throughout the beamline, the proposal for how to optimize the beamline can be developed. Some preliminary solutions have been determined such as changing the angle of the dipole magnets slightly, moving the dipole magnets transversely the misaligned distance upstream, and inserting correctors within the beamline that would bring the misaligned beam back on-axis.

9. Acknowledgements

I would like to say a special thank you to my advisors: Dr. Thomas Kroc and Dr. Carol Johnstone for their continual support throughout the duration of this project. I would also like to thank Adam Watts of the Accelerator division for his help with downloading accelerator software.

Finally, I would like to thank Dr. Elliott McCrory, Sandra Charles, Mayling L Wong-Squires, the SIST committee, and Fermi National Accelerator Laboratory for the opportunity to be a part of this program.

10. References

- [1] Hans Grote and F. Christoph Iselin. *The MAD Program User's Reference Manual*. Geneva, Switzerland, 2013.
- [2] Valeri Lebedev and J.F. Ostiguy .*The OptiMX User Guide*. Fermilab. 2014.
- [3] Fermilab. *Accelerator Report No. 4-5*. 2004.
- [4] All pictures of the Neutron Therapy Facility used with permission of Fermilab.

Appendix A: OptiMX Input File

```
# Modification of NTF_beamline short by Vazquez June 2015
$gamma=1.07053389
$Entf=($gamma-1)*$Mp
$Pcntf=sqrt((($Entf+$Mp)*($Entf+$Mp)-$Mp*$Mp)
$Hrntf=$Pcntf*1e11/$c
#Dipoles
$Rad58=58.0*$PI/180.0
$R58=60.18
$L58=60.91987
# $B58=$Hrntf/$R58 = 19.8746495
$B58Ref=$Hrntf/$R58
$B58Slp=0.005
$I58Ref=1025.
$I58=1025.
$I58Delt=$I58-$I58Ref
$B58=$B58Ref+$B58Slp*$I58Delt
$B58Angl=$Rad58*$B58Ref/$B58-$Rad58
$Bdl58Ref=$B58Ref*$L58
$Bdl58=$B58*$L58
$Bdl58kck=$Bdl58-$Bdl58Ref
$B58kck=$Bdl58kck/$B58Ref
$L58kck=1.0
$Rad32=32.0*$PI/180.0
$R32=70.8
$L32=39.54221
# $B32=$Hrntf/$R32 = 16.893452
$B32Ref=$Hrntf/$R32
$B32Slp=0.0113
$I32Ref=1057.
$I32=1057.
$I32Delt=$I32-$I32Ref
$B32=$B32Ref+$B32Slp*$I32Delt
$B32Angl=$Rad32*$B32Ref/$B32-$Rad32
$Bdl32Ref=$B32Ref*$L32
$Bdl32=$B32*$L32
$Bdl32kck=$Bdl32-$Bdl32Ref
$B32kck=$Bdl32kck/$B32Ref
$L32kck=1.0
$n58=0
$n32=0
$G58=$n58*$B58Ref/$R58
$G32=$n32*$B32Ref/$R32
$FaceAngle58=29
$FaceAngle32=16
$EffL58=3.4925
$EffL32=1.905
#quads
$ignDTL=-1.0
$ignNTF=-1.0
$Ltype5=11.38
$Ltype6=16.46
$Aptrtype5=1.7
$Aptrtype6=2.2
$Trntype5=12
$Trntype6=11
$Ktype5=8*$PI*1e-4*$Trntype5/$Aptrtype5/$Aptrtype5
$Ktype6=8*$PI*1e-4*$Trntype6/$Aptrtype6/$Aptrtype6
$QT4_30=156.4
# $QPSC01=174.6
# $QPSC02=281.9
# $QPSC03=153.3
# $QPSC04=162.4
# $QPSC05=239.7
# $QPSC06=262.3
# $QPSC07=173.9
$Pair1 = 94
$Pair2 = 100
```

```

$Pair3 = 100
$QPSC01= 176.6*$Pair1/100.
$QPSC02= 261.9*$Pair1/100.
$QPSC03= 153.3*$Pair2/100.
$QPSC04= 162.4*$Pair2/100.
$QPSC05= 239.7*$Pair3/100.
$QPSC06= 262.3*$Pair3/100.
$QPSC07= 173.9*$Pair3/100.
$GT4_30=-$ignDTL*$Ktype5*$QT4_30
$GC01= $ignNTF*$Ktype6*$QPSC01
$GC02=-$ignNTF*$Ktype6*$QPSC02
$GC03= $ignNTF*$Ktype6*$QPSC03
$GC04=-$ignNTF*$Ktype6*$QPSC04
$GC05= $ignNTF*$Ktype6*$QPSC05
$GC06=-$ignNTF*$Ktype6*$QPSC06
$GC07= $ignNTF*$Ktype6*$QPSC07
# Alignment
$ChuteOffx=0.0
$ChuteOffy=0.0
$PlateOffx=0.0
$PlateOffy=0.0
# Correctors
$IVTCTF=0.
$KVTCTF=0.2096
$GVTCTF=$KVTCTF*$IVTCTF
$K200=.0216
$ICHS1=0.
$ICHS2=$ICHS1
$GKH1=$K200*$ICHS1
$GKH2=$K200*$ICHS2
Optim
Energy[MeV]=$Entf Mass[MeV]=$Mp
Emittance: ex[cm]=0.00297 ey[cm]=0.00222 DP/P=0.004
Initial: BetaX[cm]=214.50329 BetaY[cm]=111.0188352
AlphaX=-1.230798 AlphaY=0.46795327 Qx=0 Qy=0
DispersX[cm]=0 DispersY[cm]=0
DspPrimeX=0 DspPrimeY=0
X[cm]=0.00 Y[cm]=0.00 Z[cm]=0.00 S[cm]=0.00
tetaX[deg]=-90 tetaY[deg]=0
# cell ngood plane emittance (cm-mrad), (deg-MeV) alpha beta(u) rms(u) max Design or Particle
EndCell
# 100% 90% rms(n) (cm/mrad), x or y x or y Ref.Phase Av.Phase Ref.energy
# (deg/MeV) (cm) (cm) (deg) (deg) (MeV)
# Transport finished element 13: 3. Quad
# 0 7591 x-xp 2.92689 0.31725 0.07244 0.04022 0.216488 0.2023 0.9550 0.0000 -31.6948 66.6247
66.6140
# y-yp 2.22433 0.82074 0.14623 0.29886 0.251025 0.3095 1.0290
# phi-w 6.77792 1.77629 0.37970 0.45357 21.205099 2.8375 0.0000
begin lattice. Number of periods=1
q4_30
o4_30
h4_out
K58
G58
D58
G58
o58_1
qc01
o58_2
kV
o58_3
qc02
o58_4
K32
G32
D32
G32
h32_out
o32_1
kH1
o32_2

```

```

qc03
oc03_1
kH2
oc03_2
qc04
oc04
qc05
oc05
qc06
oc06
qc07
hc7_out
oc07_tant
htant
oc_tant_tgt
htgt
oc_tgt
end lattice
#
begin list
q4_30 L[cm]=$Ltype5 G[kG/cm]=$GT4_30 Tilt[deg]=0
o4_30 L[cm]=24.971-$L58kck
h4_out Ax[cm]=1.422 Ay[cm]=1.422 Shape=1 OffsetX[cm]=0 OffsetY[cm]=0 Tilt[deg]=0
K58 L[cm]=$L58kck B[kG]=$B58kck Tilt[deg]=0
G58 B[kG]=$B58Ref Angle[deg]=$FaceAngle58 EffLen[cm]=$EffL58 Tilt[deg]=0
D58 L[cm]=$L58 B[kG]=$B58Ref G[kG/cm]=$G58
o58_1 L[cm]=25.4
qc01 L[cm]=$Ltype6 G[kG/cm]=$GC01 Tilt[deg]=0 OfsX[cm]=$PlateOffx OfsY[cm]=$PlateOffy
o58_2 L[cm]=2.64
kV L[cm]=12.5 B[kG]=$GVTCTF Tilt[deg]=90.
o58_3 L[cm]=2.64
qc02 L[cm]=$Ltype6 G[kG/cm]=$GC02 Tilt[deg]=0 OfsX[cm]=$PlateOffx OfsY[cm]=$PlateOffy
o58_4 L[cm]=20.27-$L32kck
K32 L[cm]=$L32kck B[kG]=$B32kck Tilt[deg]=0
G32 B[kG]=$B32Ref Angle[deg]=$FaceAngle32 EffLen[cm]=$EffL32 Tilt[deg]=0
D32 L[cm]=$L32 B[kG]=$B32Ref G[kG/cm]=$G32
h32_out Ax[cm]=1.905 Ay[cm]=1.905 Shape=1 OffsetX[cm]=0 OffsetY[cm]=0 Tilt[deg]=0
o32_1 L[cm]=40.8
kH1 L[cm]=20. B[kG]=$GKH1 Tilt[deg]=0.
o32_2 L[cm]=3.97
qc03 L[cm]=$Ltype6 G[kG/cm]=$GC03 Tilt[deg]=0 OfsX[cm]=$ChuteOffx OfsY[cm]=$ChuteOffy
oc03_1 L[cm]=15.4
kH2 L[cm]=20. B[kG]=$GKH2 Tilt[deg]=0.
oc03_2 L[cm]=35.72
qc04 L[cm]=$Ltype6 G[kG/cm]=$GC04 Tilt[deg]=0 OfsX[cm]=$ChuteOffx OfsY[cm]=$ChuteOffy
oc04 L[cm]=49.53
qc05 L[cm]=$Ltype6 G[kG/cm]=$GC05 Tilt[deg]=0 OfsX[cm]=$ChuteOffx OfsY[cm]=$ChuteOffy
oc05 L[cm]=39.37
qc06 L[cm]=$Ltype6 G[kG/cm]=$GC06 Tilt[deg]=0 OfsX[cm]=$ChuteOffx OfsY[cm]=$ChuteOffy
oc06 L[cm]=26.67
qc07 L[cm]=$Ltype6 G[kG/cm]=$GC07 Tilt[deg]=0 OfsX[cm]=$ChuteOffx OfsY[cm]=$ChuteOffy
hc7_out Ax[cm]=1.905 Ay[cm]=1.905 Shape=1 OffsetX[cm]=0 OffsetY[cm]=0 Tilt[deg]=0
oc07_tant L[cm]=65.24
htant Ax[cm]=0.7938 Ay[cm]=0.7938 Shape=1 OffsetX[cm]=0 OffsetY[cm]=0 Tilt[deg]=0
oc_tant_tgt L[cm]=0.9525
htgt Ax[cm]=1.27 Ay[cm]=1.27 Shape=1 OffsetX[cm]=0 OffsetY[cm]=0 Tilt[deg]=0
oc_tgt L[cm]=1.27
end list of elements
TrajParamBlock
X[cm]=0.2 Teta_X[rad]=0.
Y[cm]=-0.1 Teta_Y[rad]=0.
s[cm]=0. DeltaP/P=0.
EndTrajParamBlock

```

Appendix B: MAD8 Input File

```
!****Survey of NTF Beamline from beginning of 58 through 7th Quad****
!*****by Vazquez. Fri Jul 10 2015*****
!*****Organized by elements*****
! Kinetic energy=66.1805 MeV, mass=938.28 MeV
! BetaX=2.1649 m, AlphaX=0.04022, BetaY=2.5102 m, AlphaY=0.29886
! DispX=0 m, DispPX=0, DispY=0 m, DispPY=0
!*****Begin NTF Line*****
!*****NTF Line Quads*****
qc01: QUADRUPOLE, L= 0.1646, K1= -7.92782537
qc02: QUADRUPOLE, L= 0.1646, K1= 11.75706379
qc03: QUADRUPOLE, L= 0.1646, K1= -7.321122559
qc04: QUADRUPOLE, L= 0.1646, K1= 7.755709743
qc05: QUADRUPOLE, L= 0.1646, K1=-11.44731296
qc06: QUADRUPOLE, L= 0.1646, K1= 12.5266174
qc07: QUADRUPOLE, L= 0.1646, K1= -8.304913327
!*****NTF Line Drifts*****
o58_1: DRIFT, L=0.254
o58_2: DRIFT, L=0.0264
o58_3: DRIFT, L=0.0264
o58_4: DRIFT, L=0.1927
o32_1: DRIFT, L=0.408
o32_2: DRIFT, L=0.0397
oc03_1:DRIFT, L=0.154
oc03_2:DRIFT, L=0.3572
oc04: DRIFT, L=0.4953
oc05: DRIFT, L=0.3937
oc06: DRIFT, L=0.2667
!*****NTF Line Bends*****
D58: RBEND, L= 0.583518992, ANGLE=-1.012294284
D32: RBEND, L= 0.3903162777, ANGLE=-0.558505791
```

```

!*****Kickers*****
K58: kicker, L= 0.01,hkick=0, vkick= 0
kV:  kicker, L=0.125,hkick=0, vkick= 0
K32: kicker, L= 0.01,hkick=0, vkick= 0
kH1: kicker, L= 0.2, hkick=0, vkick= 0
kH2: kicker, L= 0.2, hkick=0, vkick= 0
!*****Beamline from Linac tank 4 to NTF line*****

NTFLINE: LINE=(D58,o58_1, qc01, o58_2, kV, o58_3, qc02, o58_4, &
K32, D32, o32_1, kH1, o32_2, qc03, oc03_1, kH2, oc03_2,&
qc04, oc04, qc05, oc05, qc06, oc06, qc07)

use,ntfline
print,range=ntfline

EOPTION, ADD
SELECT, flag=error, D58
EALIGN,DS=0.01393
SELECT, flag=error, D32
EALIGN, DS=0.01170
EPRINT, RANGE=NTFLINE
twiss, save,betx= 1.19859,alfx= 1.39781,bety= 2.08525,alfy= -2.05854
Print, range=ntfline
survey,save, z0=-0.012,x0=36.792,theta0=4.712476945,TAPE=line.survey
plot,table=twiss,colour=100,haxis=s,vaxis1=betx,bety,&
vaxis2=dx
plot,table=twiss,colour=100,haxis=s,vaxis1=betx,bety,&
vaxis2=dy

stop

```